The Upper Mantle and Transition Zone

Daniel J. Frost[*]

The upper mantle is the source of almost all magmas. It contains major transitions in rheological and thermal behaviour that control the character of plate tectonics and the style of mantle dynamics. Essential parameters in any model to describe these phenomena are the mantle's compositional and thermal structure. Most samples of the mantle come from the lithosphere. Although the composition of the underlying asthenospheric mantle can be estimated, this is made difficult by the fact that this part of the mantle partially melts and differentiates before samples ever reach the surface. The composition and conditions in the mantle at depths significantly below the lithosphere must be interpreted from geophysical observations combined with experimental data on mineral and rock properties. Fortunately, the transition zone, which extends from approximately 410 to 660 km, has a number of characteristic globally observed seismic properties that should ultimately place essential constraints on the compositional and thermal state of the mantle.

INTRODUCTION

Xenoliths and slices of the mantle emplaced tectonically into the crust show that the upper mantle is dominated by peridotite, a rock composed of olivine, clinopyroxene, orthopyroxene, and an Al-bearing phase that changes with increasing depth from plagioclase (<30 km) to spinel (30–70 km) and then to garnet (>70 km). Almost all mantle samples, however, come from the conductively cooled lithosphere. Although they were originally part of the underlying convectively cooled asthenosphere, they have generally undergone melt extraction during emplacement in the lithosphere and they often show evidence of post-emplacement metasomatism. By tracing the chemical trends that result from these processes, the likely composition of the original asthenospheric mantle can be estimated, but the scale and depth to which this estimate remains valid are uncertain.

As most mantle rock samples come from depths less than 200 km, investigating the thermal, mineralogical and chemical structure of the deeper mantle requires the interpretation of geophysical observations, primarily those from seismology, but additional constraints can be provided by gravity, electrical conductivity and heat flow measurements. The principal approach is to assume a mantle bulk composition, determine its mineralogy as a function of depth in high-pressure experiments, then calculate the sound velocities for this assemblage using mineral-physics data, and critically compare them with seismic reference models for global body wave velocity structure, such as PREM (preliminary reference Earth model) (e.g. Dziewonski and Anderson 1981).

The transition zone, between 410 and 660 km, is an excellent region to perform such a comparison because it is free of the complex thermal and chemical structure imparted on the shallow mantle by the lithosphere and melting processes. It contains a number of seismic discontinuities—sharp jumps in seismic velocity, that are generally accepted to arise from mineral phase transformations (Agee 1998). These discontinuities have certain features that correlate directly with characteristics of the mineral transformations, such as the proportions of the transforming minerals and the temperature at the discontinuity. They, therefore, provide constraints on mantle properties that complement those provided by 1-D velocity–depth models. These discontinuity features can also be determined at a local scale, and when combined with local 3-D velocity models there should ultimately be enough constraints to separate thermal from chemical variations. Although the interpretation of seismic observations has been hindered by limits in mineral-physics measurements, these have improved dramatically in recent years. Uncertainties still exist, but the quality of mineral data has to some extent shifted the focus onto the requirement for more-detailed seismic observations and reference models (e.g. Cammarano et al. 2005).

To a first approximation, the variation of S- and P-wave velocities (Vs and Vp) with depth are in reasonable agreement with a peridotitic upper mantle and transition zone. In detail, however, a number of inconsistencies remain, and there are further observations implying that the mantle may be more complex. Some observations, for example, raise questions concerning (1) the scale at which the mantle can be considered chemically homogeneous, (2) the origin of the asthenospheric low-velocity zone, (3) whether volatile-induced partial melting occurs in the deep mantle and (4) whether the transition zone might also provide at least a temporary resting place for subducted oceanic crust due to buoyancy-driven or viscosity-driven resistance to entering the lower mantle.

* Bayerisches Geoinstitut, University of Bayreuth
  Bayreuth, Germany D95447
  E-mail: Dan.Frost@uni-bayreuth.de

COMPOSITION AND MINERALOGY OF THE UPPER MANTLE AND TRANSITION ZONE

By comparing seismic properties with those estimated for particular mineral assemblages, the physical and chemical properties of the mantle can be constrained. A reasonable starting point in such an analysis is to choose an average upper-mantle chemical composition and then examine the mismatch between the seismic properties observed and calculated for a mineral assemblage reflecting this composition as a function of depth. A number of methods have been used to estimate upper-mantle composition. The simplest use analyses of xenoliths that appear to have been unaffected by melting, while others assume that certain elements in the mantle have chondritic ratios (i.e. ratios found in meteorites considered to be the unfractionated building blocks of the Earth). Pyrolite, on the other hand, a synthetic rock composition conceived by Ringwood as the source rock for mid-oceanic ridge basalts (MORB), was constructed by mixing a basalt composition with what was considered to be the corresponding mantle-melt residue (see Ringwood 1991). Differences in major-element concentrations between the majority of recently proposed upper-mantle compositions appear quite minor (Walter 2004). There are slightly more-obvious differences between the mineral proportions estimated for such compositions at, for example, 1.5 GPa (gigapascals). Most compositions result in olivine contents in the range 49–62%. Models that assume chondritic ratios for some elements have in general lower olivine contents than models based primarily on mantle samples, while pyrolite falls roughly in the middle (56%). Although the various compositions would become much more distinct if we were comparing the types of basalts they would produce by partial melting in the MORB source region, differences in terms of density and elastic properties are likely to be at the limit of what can be discriminated using geophysical observations.

FIGURE 1 shows the variation in mineral proportions of a pyrolite composition as a function of depth along an oceanic geotherm. This is most easily described by dividing the diagram in two and first describing the olivine transitions, each of which is related to a seismic discontinuity, and then transformations in the remaining Si- and Al-rich minerals, which undergo phase transformations over much broader depth intervals. The transition zone begins at ~14 GPa (410 km depth), where $(Mg,Fe)_2SiO_4$ olivine transforms into the denser structure wadsleyite, sometimes referred to as β-phase or modified spinel. At ~17.5 GPa (520 km), wadsleyite transforms into ringwoodite, sometimes termed γ-phase or silicate spinel. At approximately 24 GPa (660 km), ringwoodite breaks down to an assemblage of perovskite-structured $(Mg,Fe)SiO_3$ and $(Mg,Fe)O$ magnesiowüstite (actually ferropericlase as MgO is greater than FeO), which marks the beginning of the lower mantle. With respect to Si- and Al-rich phases, by 3 GPa pyrolite is composed of garnet peridotite, but with increasing pressure both clinopyroxene and orthopyroxene components are incorporated into garnet as a result of the garnet octahedral site, which is normally occu-

pied by Al, accepting Mg (and Fe) and Si. The Al-free garnet end member $(Mg,Fe)_4Si_4O_{12}$ is called majorite. This substitution is favoured with increasing pressure and temperature. Garnet accepts Mg and Fe into the octahedral site but not Ca, so the majorite substitution initially decreases the proportion of orthopyroxene; however by mid–transition zone conditions, all pyroxene components are hosted by garnet. At pressures higher than 18 GPa, $CaSiO_3$ perovskite starts to exsolve from garnet. At depths greater than 660 km, garnet also transforms into $(Mg,Fe)(Al,Si)O_3$ perovskite, over a wider pressure interval than the ringwoodite transformation, causing the Al content of perovskite to increase over the first 50 km of the lower mantle.

The uniformity in the major-element composition of MORB over time is apparent evidence that the upper mantle has a relatively homogeneous composition, at least at the scale at which partial melting takes place. However, trace elements and radiogenic isotopes indicate significant chemical heterogeneity in the basalt source region. These characteristics must reflect, to some extent, the more mobile nature of incompatible trace elements, while variations in major elements should be much smaller. On the other hand, certain geochemical signatures in mantle-derived magmas are widely believed to be caused by the presence of subducted oceanic crust in the mantle. In some studies, it has been proposed that partial melts from subducted crust are a component of most mantle-derived magmas and that the relative homogeneity of MORB in fact reflects mixing either in magma chambers or through melt
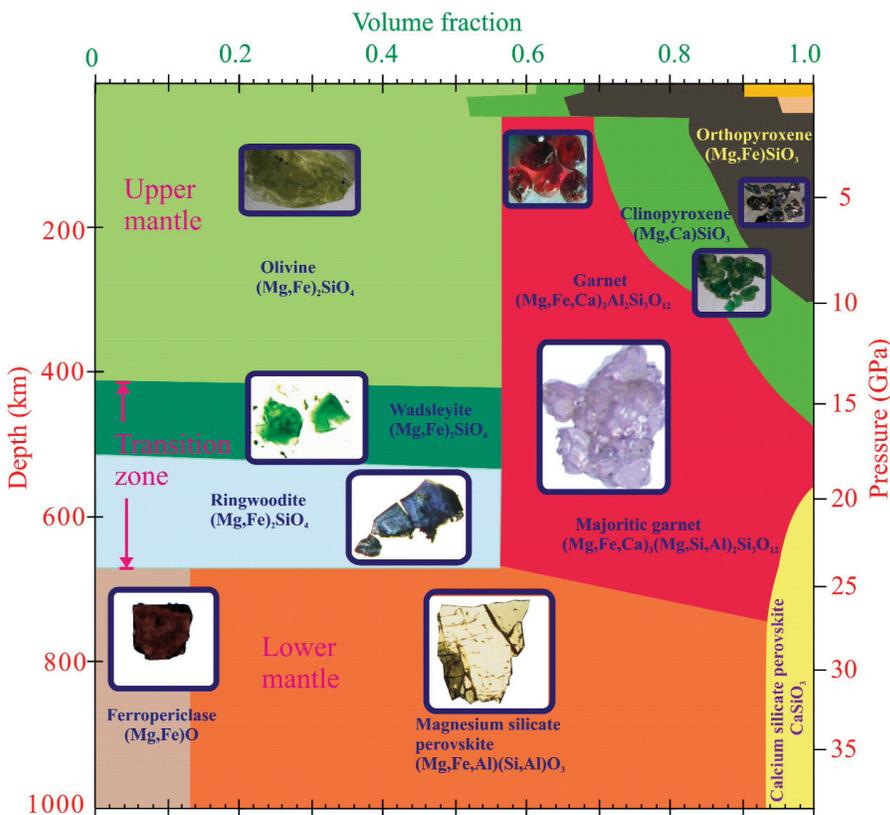
FIGURE 1 Mineral volume fractions for the top 1000 km of a pyrolite mantle. Small orange and pink regions in the top-right-hand corner denote the stabilities of feldspar and spinel, respectively (Ringwood 1991; Stixrude and Lithgow-Bertelloni 2005). Five inset images show minerals recovered from high-pressure and high-temperature experiments where the field of view is typically ~0.2 mm. The olivine, garnet and pyroxene photographs are of natural samples from peridotite xenoliths.

reactions with the surrounding mantle peridotite (e.g. Yaxley 2000; Meibom and Anderson 2003). There is also evidence from seismology for the existence of small-scale heterogeneities in the mantle that scatter seismic waves. These scatterers have characteristic sizes ranging up to those expected for sections of recycled oceanic crust (Helffrich and Wood 2001; Shearer and Earle 2004). This seems quite reasonable as there are no grounds to believe that solid-state homogenisation processes are either effective or rapid in the mantle. Chemical diffusion could only reequilibrate recycled crust once it had been either broken up or strained by convective stirring to length scales on the order of metres (Holzapfel et al. 2005). Bodies of recycled oceanic crust may, therefore, be present in sizes that range up to those of initial subduction, mixed with variably melt-depleted peridotite. This will have important implications because instead of being an equilibrium mineral assemblage, the mantle may be, to some degree, a disequilibrium mechanical mixture of rock types on a variety of length scales. In general, a mechanical mixture of oceanic crust and melt-depleted peridotite will have a mineralogy similar to that shown in FIGURE 1, but there will be some important differences. Peridotite that has undergone partial melting will be lower in Al and Ca and will have a lower Fe/Mg ratio. If the Al content is low, the $(Mg,Fe)SiO_3$ pyroxene component will not be entirely incorporated into garnet at transition zone conditions, but instead an additional phase, akimotoite [ilmenite-structured $(Mg,Fe)SiO_3$] will form at approximately 600 km. Akimotoite transforms into $(Mg,Fe)(Al,Si)O_3$ perovskite at somewhat lower pressures than ringwoodite, shifting the perovskite stability field to shallower depths compared to a pyrolite composition. The mineralogy of subducted oceanic crust in the mantle will be similar to that followed by clinopyroxene and garnet, shown in FIGURE 1. By mid–transition zone conditions, the rock will be composed almost entirely of garnet with additional stishovite, although the Al content of the garnet will be higher than for pyrolite. Because the transformation into $(Mg,Fe)(Al,Si)O_3$ perovskite involves only garnet, perovskite stability will be shifted to greater depths when compared to pyrolite. A mechanical mixture would therefore exhibit greater complexity in the conditions of the $(Mg,Fe)(Al,Si)O_3$ perovskite transformation at ~660 km compared to pyrolite.

If the mantle is mixed with varying proportions of recycled oceanic crust in varying states of homogenisation, it may show lateral chemical and seismic heterogeneity. On the other hand, it has also been proposed that the density contrast between subducted oceanic crust and peridotite may cause mantle stratification due to the accumulation of crust in regions where it becomes neutrally buoyant. It has been argued that this might happen at the base of the transition zone (see Ringwood 1991). A recently proposed mechanism for efficiently separating subducted crust from the underlying mantle may make this scenario particularly viable (Lee and Chen 2007).

SEISMIC VELOCITY STRUCTURE

Seismic reference models such as PREM (Dziewonski and Anderson 1981) provide a one-dimensional velocity–depth profile of the Earth from the inversion of seismic-wave travel-time data in addition to other constraints. In these models velocities in the Earth are described by a set of polynomial functions that operate over defined depth intervals, with the assumption that seismic discontinuities occur at certain depths. Discontinuity depths are known from seismic observations of waves that are refracted by the discontinuity or from studying additional seismic-wave arrivals that appear as a result of reflection or conversion (e.g. a P-wave to an S-wave) at the discontinuity (Shearer 2000). In addi-

tion to the depth, such studies provide information on the size of the velocity jump at the discontinuity and the sharpness, i.e. the depth interval, of the velocity contrast. These observations are not used in most seismic reference models and can, therefore, be used to place additional constraints on mantle thermal and chemical structure.

Two reference models are shown in FIGURE 2, along with a number of other models that have been refined using mineral physical data to provide the functional form of the profiles (Cammarano et al. 2005). Differences among the models arise as a result of different assumptions and the use of slightly different seismic data. In the PREM model, for
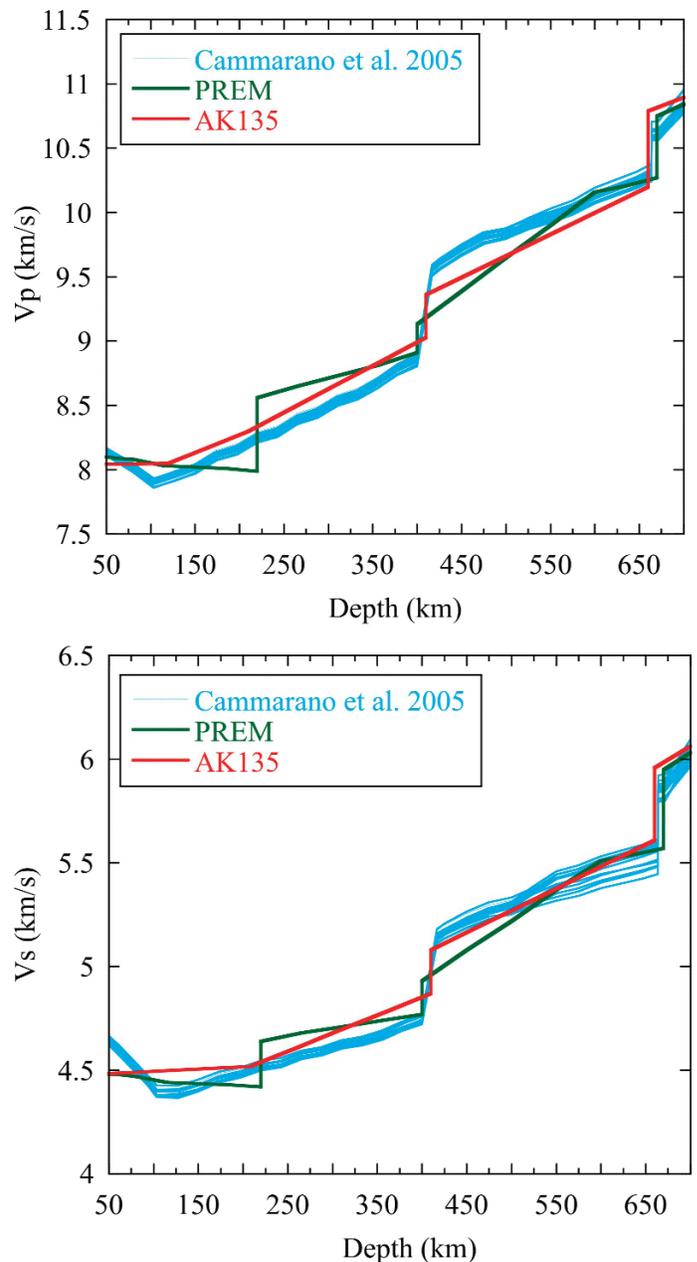
FIGURE 2 Seismic reference models PREM, AK135 and those of Cammarano et al. (2005) showing S- and P-wave velocity structure in the upper mantle and transition zone. The numerous reference models by Cammarano et al. (2005) were obtained by fitting similar global seismic data, as used in PREM, for example, to 1-D velocity models calculated for a pyrolite mineral assemblage by adjusting mineral elastic properties within the range of their uncertainties. The different models therefore arise from the use of slightly different sets of mineral properties, although all models still fit the same seismic data.

example, a discontinuity known as the Lehmann discontinuity is inferred at 220 km where it is assumed to also mark a change in seismic anisotropy. Above 220 km, seismic waves are assumed to have different speeds depending on whether they are travelling vertically or horizontally, whereas below, wave speeds are isotropic. Such behaviour can occur when minerals with strong elastic anisotropy become preferentially orientated as a result of solid-state flow. The 220 km discontinuity may therefore reflect a change in the mechanism that causes crystals to orient in the mantle, although there are other possibilities (see Deuss and Woodhouse 2004). Some later models have left out this discontinuity (e.g. Kennett et al. 1995). All models include discontinuities at approximately 410 and 660 km (hereafter termed 410 and 660), which to a first approximation match well the expected depths of the olivine to wadsleyite transition and the ringwoodite to perovskite plus ferropericlase transformation, respectively. Several weaker discontinuities, such as at 520 km (hereafter 520), which may arise from the wadsleyite to ringwoodite transformation, are absent from most reference models.

A number of studies have compared seismic reference models with S- and P-wave velocities calculated for mineral assemblages. Some studies have concluded that velocities in the transition zone are more compatible with mantle of a higher garnet/olivine ratio than pyrolite. No seismic reference model, however, is a unique fit to the global seismic data from which they are refined, due, for example, to tradeoffs between the magnitude of a discontinuity and the velocity gradients. The problem is that the underlying structure in most reference models is a series of polynomial functions with no theoretical justification. This can be rectified by fitting the same global seismic data to models calculated for actual mineral assemblages, assuming a particular bulk composition and temperature gradient (Cammarano et al. 2005). The adjustable parameters in the fitting procedure are the mineral elastic properties, which are varied only within the bounds of the experimental uncertainties. The underlying structure of the reference model is then theoretically justified. With this procedure Cammarano et al. (2005) have shown that within the bounds laid down by current mineral-physics measurements, global seismic data are consistent with a pyrolitic model for the upper mantle and transition zone. The numerous acceptable fits (shown in FIGURE 2) prescribe an intriguingly narrow range of mineral elastic properties, however, which can be tested in the future thanks to the continual improvements in mineral-physics measurements. By narrowing the experimental constraints, deviations from pyrolitic models or adiabatic gradients may well show up in global data in the future.

DISCONTINUITY DEPTHS

Depth estimates for transition zone discontinuities are obtained by analysing the travel times of seismic waves that are either reflected or converted at the discontinuity. Global variations in the depth of transition zone discontinuities, i.e. topography, have also been detected using SS precursors (Shearer 2000), which are S-waves that bounce off the underside of the discontinuity. To a first approximation this topography results from variations in mantle temperature and will depend on the pressure–temperature (Clapeyron) slopes of the causal mineral transformations, although variations in the bulk Fe/Mg ratio could also play a role. These Clapeyron slopes can be determined in high-pressure and high-temperature phase equilibria experiments, but to be useful they need to be determined with high accuracy. In situ X-ray diffraction experiments have determined precisely the pressure of these transformations

relative to the simultaneously measured densities of pressure-calibrant materials, such as gold, NaCl and MgO (e.g. Irifune et al. 1998). The use of discontinuity depths to determine temperatures requires that mineral transformations occur at equilibrium phase boundaries. While this may be reasonable in the ambient mantle, at the lower temperatures within subduction zones, nucleation and growth kinetics may cause mineral transformations to significantly overstep equilibrium boundary conditions.

SS precursors are sensitive only to large-wavelength discontinuity topography, and small-scale perturbations (<1000 km) arising from plumes or subduction zones will be averaged out. In FIGURE 3, the vertical shaded portions show the range of global topography of the 410, 520 and 660 discontinuities (Shearer 2000). In comparison, the Clapeyron slopes of the $(Mg,Fe)_2SiO_4$ olivine to wadsleyite and wadsleyite to ringwoodite transformations are shown with filled sections indicating temperatures that correspond to the observed depth variations. Five individual studies on the Mg_2SiO_4 ringwoodite to silicate perovskite plus periclase reaction are also shown. The average depth of the 410 (actually at 418 km) implies a temperature of 1480°C, but the global topography indicates a temperature variation of ±100°C. However, even though we would expect the temperature at 520 km to be at least 50° higher than at 410, due to adiabatic compression, the average value is 1390°C with a topography of ±100°C. There is a wide spread in temperatures predicted by different studies on the 660 transformation, with most studies predicting temperatures that are much lower than expected. Comparing the Clapeyron slopes of these studies with 660 topography predicts minimum variations in temperature of ±200°C, i.e. higher than at 410 or 520. The disagreements among studies on the 660
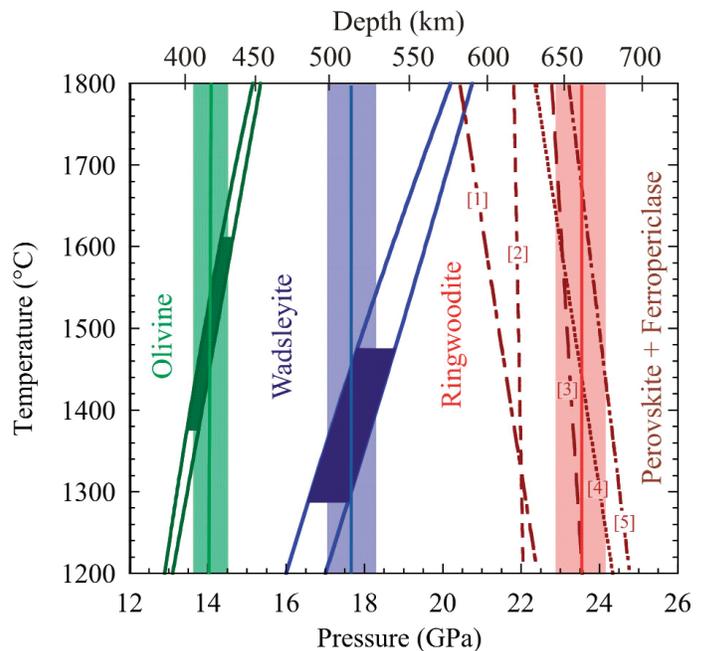
FIGURE 3 Pressure–temperature slopes for transition zone phase transformations compared to average discontinuity depths (vertical solid lines) and global topography (vertical shaded regions) of the 410 (green), 520 (blue) and 660 km (red) discontinuities. Double curves for the olivine–wadsleyite and wadsleyite–ringwoodite transformations indicate the depth intervals where transforming $(Mg,Fe)_2SiO_4$ solid solutions coexist (Frost 2003). These curves are shaded to indicate temperature ranges compatible with global discontinuity topography. The figure also shows individual curves for the Mg_2SiO_4 ringwoodite to perovskite + periclase reaction from different studies: [1] Irifune et al. (1998), [2] Katsura et al. (2003), [3] Fei et al. 2004, [4] Ito and Takahashi (1989) and [5] Shim et al. (2001).

arise principally because there is no absolute scale of pressure at these high-temperature conditions, and the equation of state for any pressure-calibrant material must be extrapolated to the conditions of the measurements. Uncertainty will therefore remain, even for studies that appear to give reasonable temperatures.

The apparent decrease in average mantle temperature between 410 and 520 might also result from imprecise experimental pressure estimates, although as opposed to the 660, multiple studies on the 410 and 520 mineral transformations are in good agreement. In addition, in the case of the 660, certain calibrants appear to underestimate the pressure, whereas for the 520 to correspond to erroneously low temperatures, similar pressure calibrants would have to be overestimating the pressure. The 520 is not observed globally, and the average depth could be easily biased if deeper signals were somehow being missed, perhaps because they become confused with the reflections from the 660. Another intriguing possibility is that average temperatures really do drop in the lower transition zone. If subducting slabs flatten out as they experience resistance to entering the lower mantle, large horizontal regions of low temperature could be present at the base of the transition zone that would raise the globally averaged "520" depth.

Recent observations of local splitting and depth variability of the 520 and 660 discontinuities might also confuse global estimates of discontinuity depths (e.g. Deuss et al. 2006). These observations are important as they might result from the presence of mechanical mixtures in the mantle comprising depleted peridotite and recycled oceanic crust.

While smaller-scale discontinuity topography is averaged out in most SS precursor studies, such topography can be detected using waves that interact with the discontinuity close to either the source or the receiver. Such studies show that the 410 is raised by over 50 km in some subduction zones, consistent with temperatures over 600°C lower than the average mantle at the same depth (Helffrich 2000).

THE SHARPNESS OF A DISCONTINUITY

Transition zone mineral phase transformations should produce velocity changes that occur over depth intervals, rather than being discontinuous step functions. This is because the transforming mantle minerals are all multi-component solid solutions with Mg and Fe end members [plus Al for $(Mg,Fe)(Al,Si)O_3$ perovskite]. The unequal partitioning of Fe and Mg causes the transforming minerals to coexist over a pressure interval. Mineral proportions will change progressively as this interval is crossed, causing a gradient in elastic properties and imparting a depth interval to the velocity jump. For a typical mantle-olivine Fe/(Fe+Mg) ratio of 0.1, the depth interval over which olivine and wadsleyite coexist at the 410 under dry conditions is shown in FIGURE 4 to be approximately 0.25 GPa or 7 km. The wadsleyite to ringwoodite transformation (i.e. 520) occurs over a broader depth interval, about 25 km, while the formation of magnesium silicate perovskite (660) is composite and results from an initial sharp transformation from ringwoodite, occurring over an interval of less than 4 km, followed by a broader transformation from garnet that occurs over 30–40 km (FIG. 1).

Studies of reflected and converted seismic waves can provide information on the depth interval over which a discontinuity occurs because high-frequency seismic waves can only be influenced by sharp velocity jumps. Global observations of high-frequency (1 Hz) reflections imply that the 660 must be ≤2 km thick, while the 410 is best modelled as a 7 km wide gradient that ends with a sharp jump (Xu et
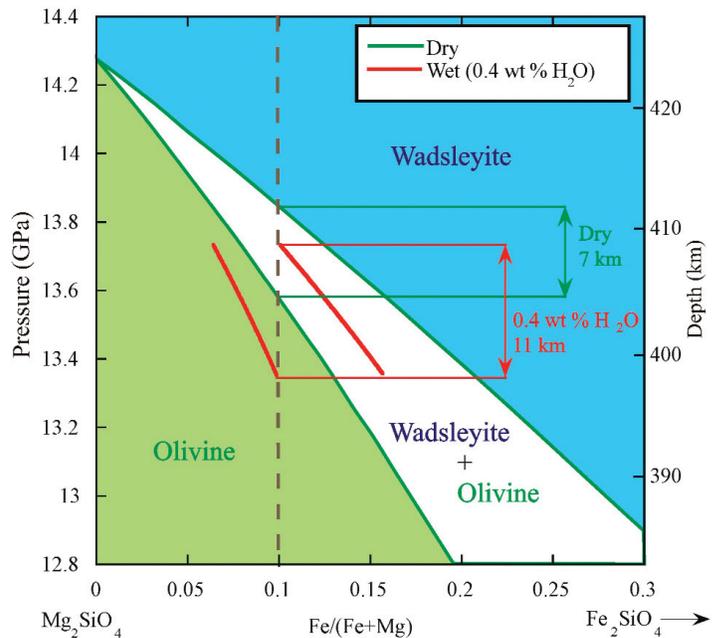
FIGURE 4 The olivine–wadsleyite transformation in the Mg_2SiO_4–Fe_2SiO_4 system calculated at 1400°C under dry conditions and with 0.4 wt% H_2O (Frost and Dolejš 2007), which is the H_2O content required to saturate olivine at these conditions. The downward displacement of the two-phase region in the hydrous system is shown by the red curves. The vertical dashed line shows a typical mantle Fe/(Fe+Mg) ratio of 0.1. The dry transition is approximately 7 km wide, while the addition of H_2O broadens the transition at these conditions to a maximum of 11 km.

al. 2003). The 520 is not observed in high-frequency studies but appears in lower-frequency observations, which is consistent with it corresponding to a gradient in velocity >10 km thick (Shearer 2000), in agreement with phase relations. Locally, however, the 410 appears to be more variable in thickness than the 660. In some localities it is apparently ≤ 4 km thick (Benz and Vidale 1993), while in other regions it may be as broad as 30 km (Van der Meijde et al. 2003). These observations might result from the presence of H_2O in the mantle (Wood 1995). Wadsleyite can accommodate the equivalent of 3 wt% H_2O as OH^- defects in its structure, and because H_2O partitions preferentially into wadsleyite over olivine, its presence will expand the wadsleyite stability field to shallower depths and broaden the two-phase region between olivine and wadsleyite. However, the solubility of H_2O in olivine and wadsleyite decreases with increasing temperature, and the effect of H_2O on the 410 is therefore relatively small at typical mantle temperatures, as shown in FIGURE 4. To produce the observed 30 km wide 410 (Van der Meijde et al. 2003) would require lower-than-average mantle temperatures (<1400°C) and large H_2O contents, consistent with levels at which olivine is H_2O saturated (Frost and Dolejš 2007). Such conditions might conceivably occur above subduction zones, where slabs have transported H_2O into the mantle. H_2O contents close to the saturation level in olivine would also be consistent with observations of low S-wave velocities just above the 410 in some regions, which could be caused by H_2O-induced partial melting (Revenaugh and Sipkin 1994).

CONCLUDING REMARKS

While measurements of mineral elastic properties are improving, new global reference models are employing mineralogical behaviour as an intrinsic component of their parameterisation. Joint inversions of travel-time data and data on waves reflected at discontinuities should result in an unprecedented ability to differentiate between chemical and thermal properties of the upper mantle and transition zone. This will require an even greater degree of collaboration between workers in petrology, mineral physics and seismology.

By performing the same types of joint inversions using regional tomographic and seismic discontinuity data, a local picture of mantle temperature and compositional variation should emerge. An important aspect in this approach will be to combine observations of seismic anisotropy in the mantle with the predictions from mineral physics for the preferred mineral alignments and elastic anisotropy of minerals. Many aspects need resolution, such as the origin of the asthenospheric low-velocity zone, whether volatiles induce partial melting in the deep mantle, and at what scale the mantle can be considered chemically homogeneous. The multiple constraints provided by different types of seismic data, however, should allow lateral variations in mantle structure to be resolved and provide key information for understanding the fundamental mechanisms that drive our remarkable Earth.

ACKNOWLEDGMENTS

REFERENCES

Agee CB (1998) Phase transformations and seismic structure in the upper mantle and transition zone. In: Hemley RJ (ed) Ultrahigh-Pressure Mineralogy. Mineralogical Society of America Reviews in Mineralogy 37, pp 165-203

Benz HM, Vidale JE (1993) Sharpness of upper-mantle discontinuities determined from high-frequency reflections. Nature 365: 147-150

Cammarano F, Deuss A, Goes S, Giardini D (2005) One-dimensional physical reference models for the upper mantle and transition zone: Combining seismic and mineral physical constraints. Journal of Geophysical Research 110: B01306, doi:10.1029/2004JB003272

Deuss A, Woodhouse JH (2004) The nature of the Lehmann discontinuity from its seismological Clapeyron slopes. Earth and Planetary Science Letters 225: 295-304

Deuss A, Redfern SAT, Chambers K, Woodhouse JH (2006) The nature of the 660-kilometer discontinuity in Earth's mantle from global seismic observations of PP precursors. Science 311: 198-201

Dziewonski AM, Anderson DL (1981) Preliminary reference Earth model. Physics of the Earth and Planetary Interiors 25: 297-356

Fei Y, Van Orman J, Li J, van Westrenen W, Sanloup C, Minarik W, Hirose K, Komabayashi T, Walter M, Funakoshi K (2004) Experimentally determined postspinel transformation boundary in Mg_2SiO_4 using MgO as an internal pressure standard and its geophysical implications. Journal of Geophysical Research 109: B02305, doi:10.1029/2003JB002562

Frost DJ (2003) The structure and sharpness of $(Mg,Fe)_2SiO_4$ phase transformations in the transition zone. Earth and Planetary Science Letters 216: 313-328

Frost DJ, Dolejš D (2007) Experimental determination of the effect of H_2O on the 410-km seismic discontinuity. Earth and Planetary Science Letters 256: 182-195

Helffrich G (2000) Topography of the transition zone seismic discontinuities. Reviews of Geophysics 38: 141-158

Helffrich GR, Wood BJ (2001) The Earth's mantle. Nature 412: 501-507

Holzapfel C, Rubie DC, Frost DJ, Langenhorst F (2005) Fe-Mg interdiffusion in $(Mg,Fe)SiO_3$ perovskite and lower mantle reequilibration. Science 309: 1707-1710

Irifune T, Nishiyama N, Kuroda K, Inoue T, Isshiki M, Utsumi W, Funakoshi K-I, Urakawa S, Uchida T, Katsura T, Ohtaka O (1998) The postspinel phase boundary in Mg_2SiO_4 determined by in situ X-ray diffraction. Science 279: 1698-1700

Ito E, Takahashi E (1989) Postspinel transformations in the system Mg_2SiO_4-Fe_2SiO_4 and some geophysical implications. Journal of Geophysical Research 94: 10637-10646

Katsura T, Yamada H, Shinmei T, Kubo A, Ono S, Kanzaki M, Yoneda A, Walter MJ, Ito E, Urakawa S, Funakoshi K, Utsumi W (2003) Post-spinel transition in Mg_2SiO_4 determined by high P–T in situ X-ray diffractometry. Physics of the Earth and Planetary Interiors 136: 11-24

Kennett BLN, Engdahl ER, Buland R (1995) Constraints on seismic velocities in the Earth from traveltimes. Geophysical Journal International 122: 108-124

Lee C-TA, Chen W-P (2007) Possible density segregation of subducted oceanic lithosphere along a weak serpentinite layer and implications for compositional stratification of the Earth's mantle. Earth and Planetary Science Letters 255: 357-366

Meibom A, Anderson DL (2003) The statistical upper mantle assemblage. Earth and Planetary Science Letters 217: 123-139

Revenaugh J, Sipkin SA (1994) Seismic evidence for silicate melt atop the 410-km mantle discontinuity. Nature 369: 474-476

Ringwood AE (1991) Phase transformations and their bearing on the constitution and dynamics of the mantle. Geochimica et Cosmochimica Acta 55: 2083-2110

Shearer PM (2000) Upper mantle seismic discontinuities. In: Karato S-I, Forte AM, Liebermann RC, Masters G, Stixrude L (eds) Earth's Deep Interior: Mineral Physics and Tomography From the Atomic to the Global Scale. Geophysical Monograph 117, pp 115-131

Shearer PM, Earle PS (2004) The global short-period wavefield modeled with a Monte Carlo seismic phonon method. Geophysical Journal International 158: 1103-1117

Shim S-H, Duffy TS, Shen G (2001) The post-spinel transformation in Mg_2SiO_4 and its relation to the 660-km seismic discontinuity. Nature 411: 571-574

Stixrude L, Lithgow-Bertelloni C (2005) Mineralogy and elasticity of the oceanic upper mantle: origin of the low-velocity zone. Journal of Geophysical Research 110, B03204, doi 10.1029/2004JB002965

Van der Meijde M, Marone F, Giardini D, van der Lee S (2003) Seismic evidence for water deep in Earth's upper mantle. Science 300: 1556-1558

Walter MJ (2004) Melt extraction and compositional variability in mantle lithosphere. In: Carlson RW (ed) Treatise on Geochemistry volume 2, The Mantle and Core. Elsevier, Amsterdam, pp 363-394

Wood BJ (1995) The effect of H_2O on the 410-kilometer seismic discontinuity. Science 268: 74-76

Xu F, Vidale JE, Earle PS (2003) Survey of precursors to P´P´: Fine structure of mantle discontinuities. Journal of Geophysical Research 108: B1,2024, doi: 10.1029/2001JB000817

Yaxley GM (2000) Experimental study of the phase and melting relations of homogeneous basalt + peridotite mixtures and implications for the petrogenesis of flood basalts. Contributions to Mineralogy and Petrology 139: 326-338